

2010

# A Study on Contact Force Between Wraps of Scroll Compressor for CO<sub>2</sub> Refrigerant

Akira Hiwata  
*Panasonic Corporation*

Kiyoshi Sawai  
*Panasonic Corporation*

Atsushi Sakuda  
*Panasonic Corporation*

Takashi Morimoto  
*Panasonic Corporation*

Mitsuhiro Fukuta  
*Shizuoka University*

*See next page for additional authors*

Follow this and additional works at: <http://docs.lib.purdue.edu/icec>

---

Hiwata, Akira; Sawai, Kiyoshi; Sakuda, Atsushi; Morimoto, Takashi; Fukuta, Mitsuhiro; and Yanagisawa, Tadashi, "A Study on Contact Force Between Wraps of Scroll Compressor for CO<sub>2</sub> Refrigerant" (2010). *International Compressor Engineering Conference*. Paper 1959. <http://docs.lib.purdue.edu/icec/1959>

This document has been made available through Purdue e-Pubs, a service of the Purdue University Libraries. Please contact [epubs@purdue.edu](mailto:epubs@purdue.edu) for additional information.

Complete proceedings may be acquired in print and on CD-ROM directly from the Ray W. Herrick Laboratories at <https://engineering.purdue.edu/Herrick/Events/orderlit.html>

---

**Authors**

Akira Hiwata, Kiyoshi Sawai, Atsushi Sakuda, Takashi Morimoto, Mitsuhiro Fukuta, and Tadashi Yanagisawa

## A Study on Contact Force between Wraps of Scroll Compressor for CO<sub>2</sub> Refrigerant

Akira HIWATA<sup>1\*</sup>, Kiyoshi SAWAI<sup>1</sup>, Atsushi SAKUDA<sup>1</sup>, Takashi Morimoto<sup>1</sup>,  
Mitsuhiro FUKUTA<sup>2</sup>, Tadashi YANAGISAWA<sup>2</sup>

<sup>1</sup>Appliances Development Center, Home Appliances Company, Panasonic Corporation  
2-3-1-2 Noji-higashi, Kusatsu, Shiga, 525-8555, Japan  
Phone: +81-50-3687-2893, Fax: +81-77-563-1967, E-mail: hiwata.akira@jp.panasonic.com

<sup>2</sup>Department of Mechanical Engineering, Faculty of Engineering, Shizuoka University  
3-5-1 Johoku, Nakaku, Hamamatsu, Shizuoka, 432-8561, Japan

\* Corresponding Author

### ABSTRACT

The CO<sub>2</sub> compressors have a lot of difficulties to reduce the leakage because of its very high operating pressure. The scroll compressor has two leakage passes, which are the gap in an axial direction at the tip of the wrap and the gap in a radial direction between the wraps. Many attempts to reduce the leakage through those gaps have been actively researched and developed. In this study, we grasped the characteristics of the contact force between the wraps of a CO<sub>2</sub> scroll compressor with the fixed-radius crank mechanism by measuring the oil-film pressure at the main bearing. As a result, we found that (1) there is a fluctuation of the contact force at one revolution, (2) the contact force increases with rotational speed and (3) contact force increases with decreasing the wrap clearance ratio.

### 1. INTRODUCTION

The various approaches to prevent leakage of refrigerant during compression have been reported, paying attention to the axial gap and the radial gap which are two major leakage passes of the scroll compressor. Regarding the technology for preventing leakage at the radial gap, the research of building up the dynamics model for each case of the fixed-radius crank mechanism and the variable-radius crank mechanism, and then analytically grasping and comparing the contact force which operates between wraps in the radial direction have been reported (Morishita *et al.*, 1985). However, regarding the contact force, it is considered that the gaps of an eccentric bearing and a main bearing as well as oil film formation will change due to contact of the wrap of the orbiting scroll with the wrap of the fixed scroll. No detailed research about those characteristics is reported. In this study, the characteristics and mechanism of the contact force acting between wraps have been investigated experimentally by measuring the oil film pressure distribution in the main bearing, with regard to the scroll compressor for CO<sub>2</sub> refrigerant with the fixed-radius crank mechanism.

### 2. STRUCTURE OF THE SCROLL COMPRESSOR

We used the CO<sub>2</sub> scroll compressor for heat pump water heater in this study (Hiwata *et al.*, 2002). It has been adopting the high-pressure vessel, in which the refrigerant in the suction chamber is compressed and then discharged into the vessel. Further, the seal ring is provided between the end plate surface at the anti-compression chamber side of the orbiting scroll and the frame, and it is dividing the high pressure part and the middle pressure part. This middle pressure part fulfils the role of preventing leakage of the refrigerant during compression, by pressing the orbiting scroll toward the fixed scroll and so decreasing the gap at the tip of the wrap. Further, the sub frame is provided at the lower part inside the vessel. The stator of the motor is fixed between the sub frame and the frame that constitutes the compression mechanism, by means of press fit and welding, etc. at the inner face of the vessel,

and the rotor of the motor is supported at the inner face of the stator. Moreover, the crankshaft is penetrating through the center of the rotor, and the crankshaft is supported by the both frames.

### 3. DEFINITION OF FORCES

Figure 1 shows the schematic diagrams and definition of the forces regarding the main bearing part (a), eccentric bearing part (b) and wrap contact area (c) of the crankshaft in the case that the wraps of the orbiting scroll and fixed scroll come into contact with each other. It is defined that the direction of eccentricity at the eccentric shaft part of the crankshaft is  $x$ -axis, a direction of  $90^\circ$  from the  $x$ -axis in the clockwise rotation is  $y$ -axis, and a rotating direction of the crankshaft is counterclockwise. When focusing on the eccentric bearing part, the tangential force  $F_t$ , radial gas force  $F_r$ , centrifugal force of the orbiting scroll  $F_c$  and contact force between wraps  $F_w$  act onto the orbiting scroll in addition to the oil film forces  $F_{PX1}$ ,  $F_{PY1}$  which are generated at the eccentric bearing. From above, supposing that the direction shown in Figure 1 is positive, when organizing the balance of force acting on the orbiting scroll with respect to the  $x$ -axis and the  $y$ -axis, the following equations are obtained.

$$F_c - F_r + F_{PX1} - F_w = 0 \quad , \quad F_t - F_{PY1} = 0 \quad (1)$$

On the other hand, when focusing on the main bearing part, the forces  $R_{PX1}$ ,  $R_{PY1}$  which act on the main bearing part due to the reaction force of oil film generated at the eccentric bearing part, the forces of oil film  $F_{PX2}$ ,  $F_{PY2}$  which are generated at the main bearing, and the centrifugal force  $F_{BW}$  of the crankshaft and the rotor operate. From above, supposing that the direction as shown in Figure 1 is positive, when organizing the balance of force acting on the main bearing part of the crankshaft with respect to the  $x$ -axis and the  $y$ -axis, the following equations are obtained.

$$-R_{PX1} - F_{BW} + F_{PX2} = 0 \quad , \quad R_{PY1} - F_{PY2} = 0 \quad (2)$$

Since the scroll compressor which is the subject of this study is provided with the sub frame, the sub bearing part is formed. Then, the forces  $R_{PX1}$ ,  $R_{PY1}$  in the equation (2) which act on the main bearing part due to the reaction force of oil film generated at the eccentric bearing part have been determined as the following equations, by considering the moment balance based on the sub bearing part:

$$R_{PX1} = (L_a + L_b)/L_a \cdot F_{PX1} \quad , \quad R_{PY1} = (L_a + L_b)/L_a \cdot F_{PY1} \quad (3)$$

where,  $L_a$  shows a distance between the sub bearing and the main bearing, and  $L_b$  shows a distance between the main bearing and the eccentric bearing. The reaction force at the sub bearing part has been omitted because it is sufficiently smaller than the other forces.

Next, the method for calculating the contact force  $F_w$  between wraps by using the distribution of oil film force at the main bearing part is explained. Regarding the main bearing part (a), a detail of the forces generated by the forces in the  $y$ -axis direction and by oil film is shown in Figure 2.  $\alpha_2$  shows the angle between the position where oil film becomes the minimum thickness and the  $y$ -axis. On the other hand, since the tangential force  $F_t$  acting on the orbiting scroll is the rotational force that rotates counterclockwise, the force  $R_{PY1}$  that acts on the main bearing part due to the reaction force of oil film at the eccentric bearing part is also the rotational force that rotates counterclockwise, from the equations (1), (2), (3). As the result, the oil film pressure distribution is formed at the bearing part which has a peak of pressure at the rotating direction side compared with the position having the oil film with the minimum thickness. The angle between the direction of the resultant force  $F_{P2}$  of oil film which is the integration of this oil film pressure distribution and  $\alpha_2$  is called the angle of eccentricity  $\beta_2$ . Here, since  $\alpha_2 - \beta_2$  represents a delay of the angle against the tangential force, it is called the delay angle  $\gamma_2$  of oil film's resultant force, in this study. When representing the relationship between the resultant force  $F_{P2}$  of oil film and the oil film forces  $F_{PX2}$ ,  $F_{PY2}$  generated at the main bearing part by using this delay angle  $\gamma_2$  of oil film's resultant force, the following equations are obtained.

$$F_{PX2} = F_{P2} \cdot \sin \gamma_2 \quad , \quad F_{PY2} = F_{P2} \cdot \cos \gamma_2 \quad (4)$$

From the equations (1), (2), (3), and (4), the oil film forces  $F_{PX1}$ ,  $F_{PX2}$  in the  $x$ -axis direction generated at the main bearing part and the eccentric bearing part are expressed as follows.

$$F_{PX1} = L_a / (L_a + L_b) \cdot (F_{PX2} - F_{BW}) \quad , \quad F_{PX2} = (L_a + L_b) / L_a \cdot F_t \cdot \tan \gamma_2 \quad (5)$$

Then, from the equations (1) and (5), the contact force  $F_w$  between wraps can be expressed by the following equations.

$$F_w = F_c - F_r - L_a / (L_a + L_b) \cdot F_{BW} + F_t \cdot \tan \gamma_2 \quad (6)$$

In the equation (6), since the radial gas force  $F_r$ , centrifugal force of the orbiting scroll  $F_c$ , and centrifugal force of the crankshaft and rotor  $F_{BW}$  are the values which can be theoretically calculated, it is possible to calculate the contact force  $F_w$  between wraps, by experimentally obtaining the tangential force  $F_t$  and the delay angle  $\gamma_2$  of oil film's resultant force at the main bearing part.

### 4. ESTIMATION METHOD OF CONTACT FORCE

In the previous chapter, it has been shown that measurement of the tangential force  $F_t$  and the delay angle  $\gamma_2$  of oil film's resultant force at the main bearing part is necessary to calculate the contact force  $F_w$  between wraps. In this chapter, a method of the experiment for the tangential force  $F_t$  and the delay angle  $\gamma_2$  of oil film's resultant force at the main bearing part is explained.

#### 4.1 Estimation Method of Tangential Force $F_t$

The tangential force  $F_t$  consists of a sum of the tangential gas force  $F_{tg}$  and tangential friction force  $F_{tf}$ . Then, a loss analysis of the scroll compressor for CO<sub>2</sub> refrigerant using an indicated diagram was performed (Shiibayashi *et al.*, 1988 and Shimoji *et al.*, 2008). Therefore, tangential friction force  $F_{tf}$  was calculated while separating the mechanical loss  $W_{th}$  generated at the thrust bearing part. From the above, the tangential force  $F_t$  is expressed as the following equation, by using gas compression power  $W_g$  and the mechanical loss  $W_{th}$  at the thrust bearing part:

$$F_t = F_{tg} + F_{tf} = (W_g + W_{th}) / (2\pi \cdot r_0 \cdot f) \quad (7)$$

where,  $f$  is the rotational speed of the compressor.

#### 4.2 Measuring Method of the Delay Angle $\gamma_2$

In order to measure the delay angle  $\gamma_2$  of oil film's resultant force at the main bearing part, a compressor was manufactured experimentally in which the pressure sensor and gap sensor were fitted to the frame. Figure 3 shows

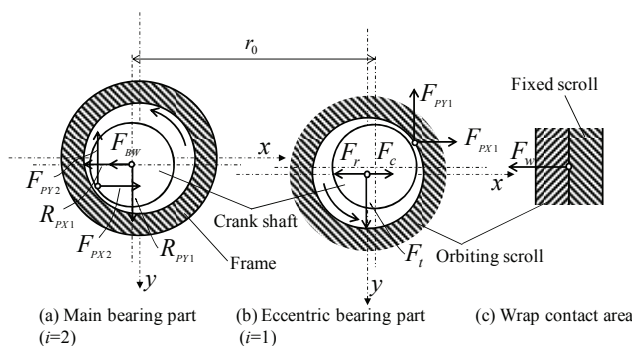
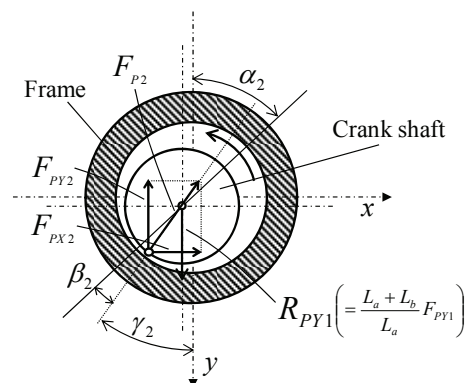


Figure 1 Definition of forces acting on (a) main bearing part, (b) eccentric bearing part and (c) wrap contact area



(a) Main bearing part ( $i=2$ )  
Figure 2 Detailed schematic diagram of y-axis forces and oil-film pressure forces

the cross sectional view of the compression mechanism in which each sensor has been inserted. Regarding the pressure sensor, the four Piezo-type pressure sensors in total with the margins to be processed at the tips were inserted into the main bearing part, being equally distributed by  $90^\circ$  pitch in the circumferential direction, and they underwent finish processing together with the inner surface of the main bearing. Moreover, the O-rings were provided near the tip of the pressure sensors so that the oil at the main bearing part shall not leak into the vessel. On the other hand, regarding the gap sensor, a target formed by a groove was processed in the crankshaft to enable detection of the crank angle. Figure 4 shows an example of the measured result of the pressure sensors and the gap sensor. The horizontal axis in Figure 4 shows the crank angle  $\theta_g$  when the output peak value of the gap sensor has been taken as a reference ( $= 0^\circ$ ), and the vertical axis shows the pressure and the gap sensor's output value when the pressure inside the vessel has been taken as a reference. Since four pressure sensors in total were fitted at equal distribution by  $90^\circ$  pitch in the circumferential direction, the four peaks can be confirmed within the range of  $360^\circ$  of the crank angle  $\theta_g$ . Further, the dotted lines in Figure 4 show the crank angles ( $=$  the directions to which the tangential force  $F_t$  operates) corresponding to the  $y$ -axis, at each position of the pressure sensors. Also, solid lines show the area centers of the pressure distribution of the pressure sensors. The delay angle  $\gamma_2$  of oil film's resultant force can be obtained as a difference in angle between these dotted line and solid line. By above study, it becomes possible to calculate the contact force  $F_w$  between wraps, with respect to the crank angle for each  $90^\circ$ .

## 5. EXPERIMENTAL CONDITIONS AND DEFINITION OF WRAP CLEARANCE

### 5.1 Experimental Conditions

The experimental conditions are shown in Table 1. Regarding these experimental conditions, the two conditions including a condition of pressure ratio and discharge temperature which is most frequently appeared throughout a year, and a condition with high pressure ratio and high discharge temperature among the operating conditions were selected. Here,  $P_d$  is a discharge pressure,  $P_s$  is a suction pressure,  $P_d / P_s$  is a pressure ratio, and  $T_d$  is a discharge temperature. The Conditions 1 – 4 have a pressure ratio of 2.5 and different rotational speeds  $f$ , and the Conditions 5 and 6 have a pressure ratio of 3.3 and different rotational speeds  $f$ .

Table 1: Experimental conditions

	$P_d / P_s$	$T_d$ [ $^\circ\text{C}$ ]	$f$ [ $\text{s}^{-1}$ ]		$P_d / P_s$	$T_d$ [ $^\circ\text{C}$ ]	$f$ [ $\text{s}^{-1}$ ]
Condition 1	2.5	95	65	Condition 4	2.5	95	30
Condition 2	2.5	95	47	Condition 5	3.3	110	65
Condition 3	2.5	95	40	Condition 6	3.3	110	51

### 5.2 Definition of Wrap Clearance and Wrap Clearance Ratio

In order to grasp the characteristics of contact force  $F_w$  acting between wraps of the scroll compressor which has adopted the fixed-radius crank mechanism, the orbiting radius  $r_o$  of the crankshaft was changed. Here, since the orbiting scroll is restricted its movement in the direction of eccentricity due to contact between wraps, it is

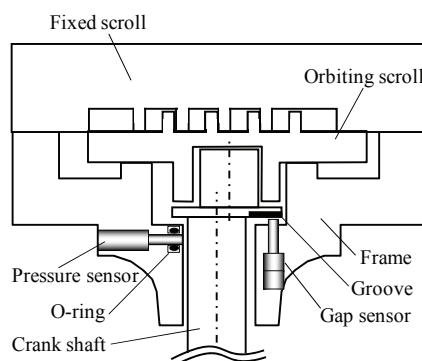


Figure 3 Cross sectional view of compression mechanism with pressure and gap sensor

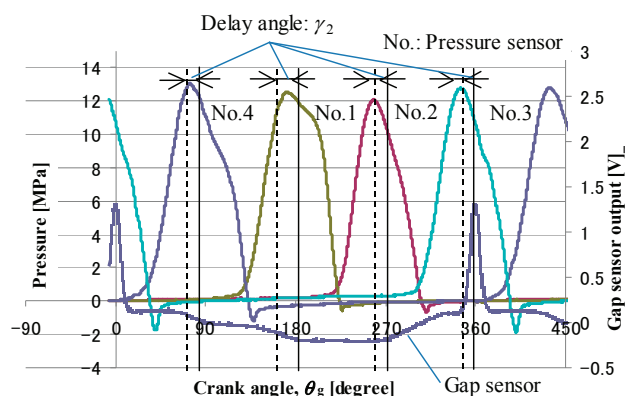


Figure 4 An experimental result of pressure sensor and gap sensor

considered that formation of bearing gaps at the eccentric bearing part and the main bearing part are also affected. Then, in this study, the wrap clearance  $C_w$  and the wrap clearance ratio  $C_w^*$  are introduced as parameters by which each bearing clearance and the orbiting radius can be considered simultaneously, and the following definition is made:

$$C_w = C_1 + C_2 + r_{0\_IDEAL} - r_0 \quad , \quad C_w^* = C_w / (C_1 + C_2) \quad (8)$$

where,  $C_1$  is a radial clearance of the eccentric bearing part,  $C_2$  is a radial clearance of the main bearing part, and  $r_{0\_IDEAL}$  is a theoretical orbiting radius which is geometrically determined from the thickness of a scroll wrap and from the base circle radius of an involute curve.

## 6. EXPERIMENTAL RESULTS AND DISCUSSIONS

### 6.1 Contact Force during One Revolution

Figure 5 shows the measured results of the contact force ratio  $F_w^*$  versus the crank angle  $\theta$  regarding the Conditions 1 – 6, when the rotation angle is taken as a reference ( $= 0^\circ$ ) where the starting position of an involute curve at the outer wall's involute of the orbiting scroll coincides with the direction of the crankshaft's eccentricity. Here, the contact force ratio  $F_w^*$  denotes the value of the contact force  $F_w$  divided by tangential force  $F_t$  of each condition ( $F_w^* = F_w / F_t$ ). Further, the wrap clearance ratio  $C_w^*$  has been fixed at 0.88. Moreover, the four pressure sensors are referred to as No.1 for the crank angle  $\theta$  of  $0^\circ$ , No.2 for the crank angle  $\theta$  of  $90^\circ$ , No.3 for the crank angle  $\theta$  of  $180^\circ$ , and No.4 for the crank angle  $\theta$  of  $270^\circ$ . As can be seen from Figure 5, the tendency has been confirmed that the contact force ratio  $F_w^*$  takes the maximum value at a crank angle  $\theta$  of  $0^\circ$  and the minimum value at  $180^\circ$ , regardless of the conditions. Further, it has been found that the maximum value of the contact force  $F_w$  is almost 20 – 30% of the tangential force  $F_t$ .

Figure 6 shows the oil film pressure distribution measured by each pressure sensor. The horizontal axis of Figure 6 corresponds to the relative crank angle  $\theta^*$  that is based on the angle at which the tangential force  $F_t$  operates at each position of the pressure sensors. The wrap clearance ratio  $C_w^*$  is 0.88, Condition 1 is fixed as the operating condition. From Figure 6, the pressure waveform at the pressure sensor No.3 has a smaller relative crank angle which becomes the area center of pressure distribution, compared with the pressure waveform at the No.1 pressure sensor, and since the delay angle  $\gamma_2$  of oil film's resultant force in Figure 2 is small, it has been found that the component in the  $x$ -axis direction of oil film force as well as the contact force  $F_w$  have become small.

Next, the reason why the contact force  $F_w$  changes during one revolution as shown in Figure 5 is observed by introducing the wrap clearance ratio  $C_{w\_OP}^*$  at operation. The wrap clearance ratio  $C_w^*$  defined by the equation (8) is based on the dimensions and the shape at assembling. However, at operation, it is supposed that the wrap clearance ratio  $C_w^*$  is changed compared with the state at assembling, due to a temperature rise of the compression mechanism. Then, when putting the wrap clearance ratio at operation as  $C_{w\_OP}^*$ , the  $C_{w\_OP}^*$  can be expressed by the following

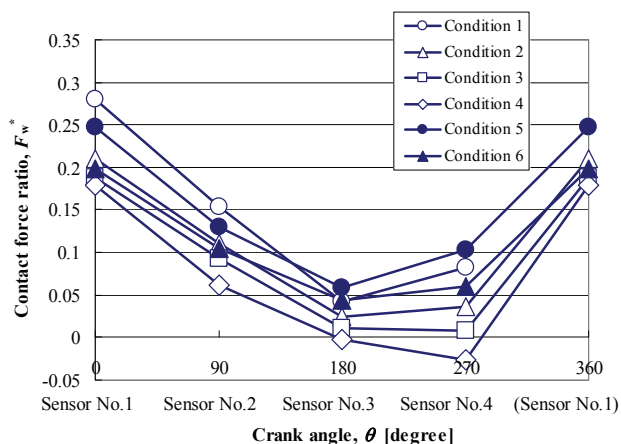


Figure 5 Relationship between contact forces and crank angle at Condition 1 – 6

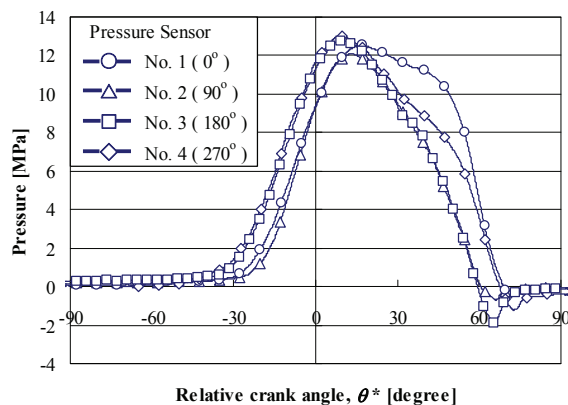


Figure 6 Oil film pressure distribution for each pressure sensor at Condition 1

equation, using the wrap clearance ratio  $C_w^*$  at assembling and the change of wrap clearance ratio  $\delta C_w^*$ :

$$C_{w\_OP}^* = C_w^* + \delta C_w^* \quad (9)$$

Here, the change of wrap clearance ratio  $\delta C_w^*$  at operation has been calculated, considering the temperature and the expansion coefficient of the fixed scroll and the orbiting scroll during operation (Yoshida *et al.*, 2008). Figure 7 shows the position of contact points between wraps of the both scroll parts when the crank angle  $\theta$  is at  $0^\circ$ . Further, Figure 8 shows the traced result of the minimum value of the change of wrap clearance ratio  $\delta C_w^*$ , by calculating the change of wrap clearance ratio  $\delta C_w^*$  at operation for each contact point as shown in Figure 7 with respect to each crank angle  $\theta$ . As shown in Figure 8, it has been found that the change of wrap clearance ratio  $\delta C_w^*$  at operation changes during one revolution.

On the other hand, the relationship between the contact force  $F_w$  and the wrap clearance ratio  $C_{w\_OP}^*$  at operation is explained by using Figure 1 and Figure 2. As the wrap clearance ratio  $C_{w\_OP}^*$  at operation becomes smaller, the crankshaft is moved toward the negative direction of the  $x$ -axis within the main bearing clearance. As the result, the delay angle  $\gamma_2$  of oil film's resultant force becomes larger, since  $\alpha_2$  becomes larger. When the tangential force  $F_t$  is almost constant, the contact force  $F_w$  becomes larger if the wrap clearance ratio  $C_{w\_OP}^*$  at operation becomes smaller. According to the abovementioned observation, the reason why the contact force  $F_w$  changes during one revolution is assumed that; the contact force  $F_w$  becomes larger by decrease of the wrap clearance ratio  $C_{w\_OP}^*$  during operation at the crank angle  $\theta$  of  $0^\circ$ , and the contact force  $F_w$  becomes smaller by increase of the wrap clearance ratio  $C_{w\_OP}^*$  during operation at the crank angle  $\theta$  of  $90^\circ$  to  $180^\circ$ .

## 6.2 Contact Force at rotational speed change

Figure 9 shows the result of summary about the contact force ratio  $F_w^*$  with regard to each pressure sensor when the rotational speed  $f$  has been changed. Here, the Conditions 1 – 4 are selected as operating conditions, and the consideration has been made so that the tangential force  $F_t$  becomes almost constant. As can be seen from Figure 9, it has been found that the contact force ratio  $F_w^*$  becomes larger when rotational speed  $f$  is increased.

Figure 10 shows the oil film pressure distribution when rotational speed  $f$  has been changed. Here, the horizontal axis of Figure 10 corresponds to the relative crank angle  $\theta^*$  that is based on the angle at which the tangential force  $F_t$  operates. The wrap clearance ratio  $C_w^*$  is 0.88. As can be seen from Figure 10, the angle position where oil film pressure becomes the maximum value remains almost the same even if rotational speed  $f$  has been changed. However, it can be confirmed that when rotational speed  $f$  is increased, the pressure buildup from a reference pressure delays at the oil film pressure rising part, and the pressure decrease delays after the oil film pressure has become the maximum value. Since the contact pressure  $F_w$  is calculated from the delay angle  $\gamma_2$  of oil film's resultant force, it has been confirmed from the detected result of waveform's distortion of the oil film pressure, that the contact force  $F_w$  is increased when rotational speed  $f$  becomes faster.

## 6.3 Contact Force at a Change of Wrap Clearance Ratio

Figure 11 shows the measured result of the contact force ratio  $F_w^*$  for Conditions 1 – 6 at pressure sensor No. 1, when the wrap clearance ratio  $C_w^*$  has been changed. Especially for the pressure sensor No.1 in which the contact

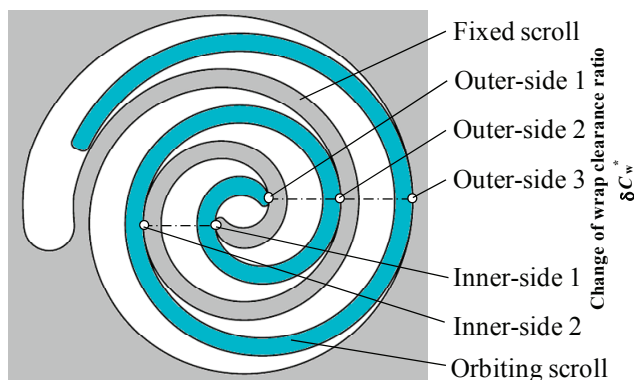


Figure 7 Definition of wrap contact points

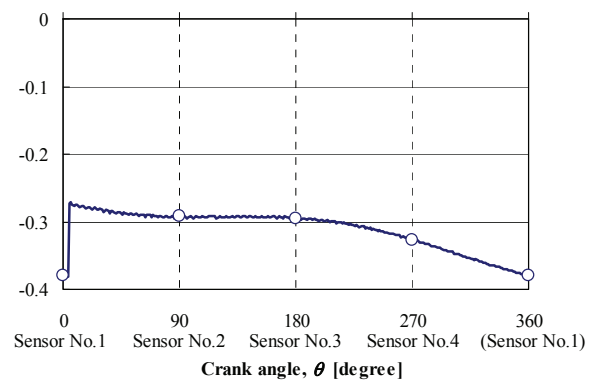


Figure 8 Change of wrap clearance ratio at Condition 1

force takes the maximum value during one revolution, a rough tendency is observed that the contact force ratio  $F_w^*$  is increased when the wrap clearance ratio  $C_w^*$  is decreased. Further, the almost same tendency has been confirmed for other pressure sensor even if the operating conditions (Conditions 1 – 6) have been changed.

Figure 12 shows the oil film pressure distribution for Condition 1 when the wrap clearance ratio  $C_w^*$  has been changed. Here, the horizontal axes of Figure 12 corresponds to the relative crank angle  $\theta^*$  that is based on the angle at which the tangential force  $F_t$  operates. Values of the delay angle  $\gamma_2$  of oil film's resultant force are shown in the explanatory note in each diagram, at the same time. It has been found that when the wrap clearance ratio  $C_w^*$  is decreased, the relative angle position of the area center in pressure distribution delays and the delay angle  $\gamma_2$  of oil film's resultant force is increased, except for the case in which the delay angle  $\gamma_2$  of oil film's resultant force has taken almost the same value when the values of wrap clearance ratio  $C_w^*$  are 0.75 and 0.88. From this result, it has been found that the change of the wrap clearance ratio  $C_w^*$  affects oil film formation at the main bearing.

### 7. CONCLUSIONS

Regarding the scroll compressor for CO<sub>2</sub> refrigerant which has used the fixed-radius crank mechanism, the characteristics of the contact force acting between wraps of the orbiting scroll and the fixed scroll have been investigated by measuring the oil film pressure which has been generated at the main bearing, and the following conclusion has been obtained.

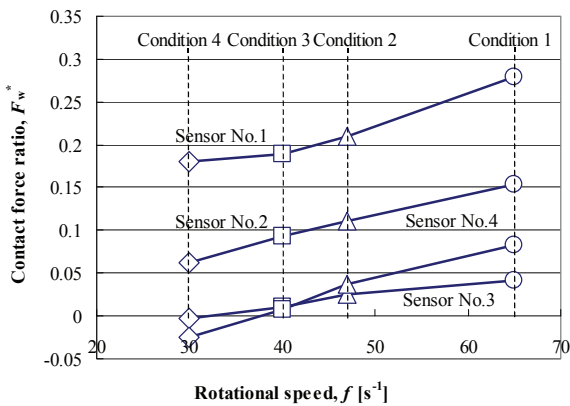


Figure 9 Relationship between contact forces and rotational speed at Condition 1 - 4

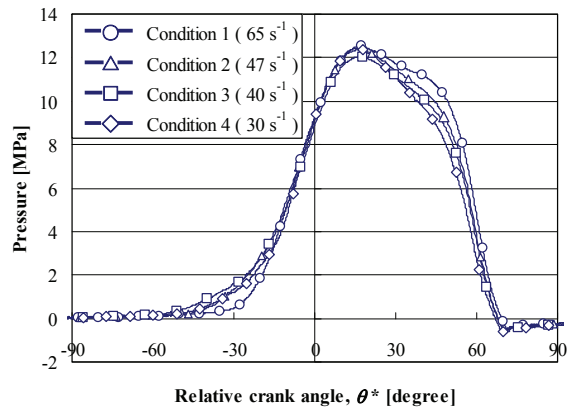


Figure 10 Oil film pressure distribution at pressure sensor No.1

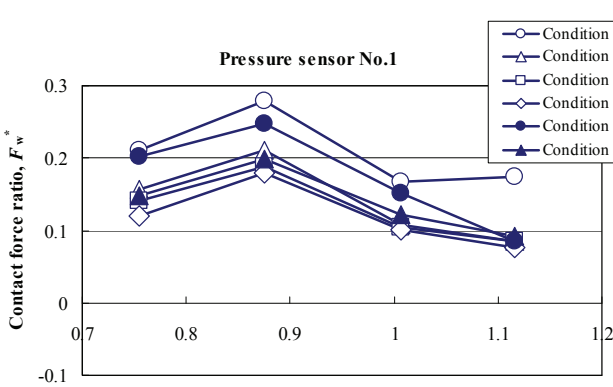


Figure 11 Relationship between contact forces and wrap clearance at Condition 1-6

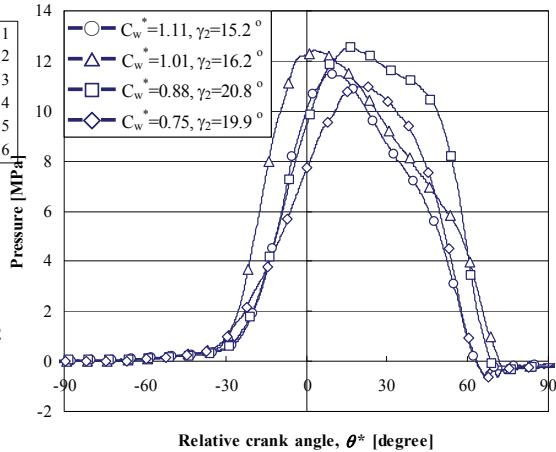


Figure 12 Oil film pressure distribution at pressure sensor No. 1 and Condition 1

- It has been clarified that the contact force acting between wraps can be calculated by measuring the delay angle of oil film's resultant force at the main bearing and tangential force.
- The maximum value of the contact force is almost 20 – 30% of the tangential force.
- Variation of the contact force during one revolution has been experimentally confirmed.
- It is assumed that the variation of the contact force during one revolution is caused by the variation of wrap clearances at operation.
- It has been confirmed from the detected result of waveform's distortion of oil film pressure, that the contact force is increased when rotational speed becomes faster, despite that the position of the maximum oil film pressure is not changed.
- The tendency has been confirmed that when a wrap clearance has been decreased, the contact force has been increased because the movement of the orbiting scroll is restricted.

## NOMENCLATURE

$C_1, C_2$	Radial clearance of eccentric bearing and main bearing	( m )
$C_w^*$	Wrap clearance ratio at assembling	( - )
$C_{w\_OP}^*$	Wrap clearance ratio at operation	( - )
$f$	Rotational speed	( s <sup>-1</sup> )
$F_c$	Centrifugal force of orbiting scroll	( N )
$F_{BW}$	Centrifugal force of crank shaft and rotor	( N )
$F_r$	Radial gas force	( N )
$F_t$	Tangential force	( N )
$F_w$	Contact force	( N )
$F_w^*$	Contact force ratio	( - )
$P_d$	Discharge pressure	( MPa )
$P_s$	Suction pressure	( MPa )
$r_0$	Orbiting radius	( m )
$r_{0\_IDEAL}$	Theoretical orbiting radius	( m )
$T_d$	Discharge temperature	( °C )
$W_g$	Gas compression power	( W )
$W_{th}$	Thrust bearing mechanical power	( W )
$\gamma_2$	Delay angle of oil-film pressure	( rad )
$\delta C_w^*$	Change of wrap clearance ratio	( - )
$\theta$	Crank angle	( rad )
$\theta^*$	Relative crank angle	( rad )

## REFERENCES

- Hiwata, A., Iida, N., Futagami, Y., Sawai, K., Ishii, N., 2002, Performance Investigation with Oil-injection to Compression Chambers on CO<sub>2</sub> -Scroll Compressor, *Proc. of 16<sup>th</sup> Int. Compressor Engineering Conf. at Purdue*, C18-4
- Morishita, E., Sugihara, M., Nakamura, T., 1985, Scroll Compressor Dynamics: 1st Report, the Model for the Fixed Radius Crank, *Trans. of the JSME*, B 51(466) pp.1981-1987
- Morishita, E., Sugihara, M., Inaba, T., Kimura, T., 1985, Scroll Compressor Dynamics: 2nd Report, the Compliant Crank and the Vibration Model, *Trans. of the JSME*, B 51(466) pp.1988-1993
- Shiibayashi, M., Tojo, K., Arata, T., Uchikawa, N., 1988, Study of Working Forces on the Orbiting Scroll and Behavior of the Scroll based on the Indicator Diagram Analysis, *Trans. of the JAR*, Vol.5, No.2, pp.53-64
- Shimoji, H., Ishizono, F., Sugawa, M., Nakamura, T., Sakai, T., Kakuda, M., Sekiya, S., Koda, T., 2008, Performance of a Double-sided Scroll Compressor for CO<sub>2</sub> Refrigerant, *Proc. of 2008 JSARE Annual Conf.*, B324
- Yoshida, H., Sakuda, A., Futagami, Y., Morimoto, T., Ishii, N., 2008, Clearance Control of Scroll Compressor for CO<sub>2</sub> Refrigerant, *Proc. of 19<sup>th</sup> Int. Compressor Engineering Conf. at Purdue*, 1251